DOI: https://doi.org/10.14256/JCE.3065.2020

Građevinar 4/2023

Primljen / Received: 22.9.2020.
Ispravljen / Corrected: 8.9.2021.
Prihvaćen / Accepted: 11.4.2022.
Dostupno online / Available online: 10.5.2023.

Innovative method for incremental dynamic analysis curves in semi-isolated bridges

Authors:

Assist.Prof. **Hamid Ganjehei**, PhD. CE
Islamic Azad University, Tehran, Iran
Department of civil engineering, Science and Research Branch
h.ganjehei@srbiau.ac.ir

Assist.Prof. **Panam Zarfam**, PhD. CE
Islamic Azad University, Tehran, Iran
Department of civil engineering, Science and Research Branch
zarfam@srbiau.ac.ir
Corresponding author

Prof. **Mohsen Ghafory-Ashtiany**, PhD. CE
International Institute of Earthquake Engineering and Seismology, Tehran, Iran
ashtiany@iiees.ac.ir

Original research paper

Hamid Ganjehei, Panam Zarfam, Mohsen Ghafory-Ashtiany

Innovative method for incremental dynamic analysis curves in semi-isolated bridges

This paper proposes an innovative method for determining the approximate incremental dynamic analysis curves of semi-isolated bridges, including the derivation of statistical mathematical formulas. Ultimately, an innovative method is devised based on the primary and limit state tangential stiffness values of semi-isolated bridges. The bridges selected for this study are two reinforced concrete highway bridges in the United States, which have been optimally re-designed using lead rubber bearing isolators. The established procedure can be used in future studies to extract the probabilistic responses of semi-isolated bridges via a simplified and efficient method.

Key words:
semi-isolated bridge, seismic evaluation, modal incremental dynamic analysis, incremental dynamic analysis

Izvorni znanstveni rad

Hamid Ganjehei, Panam Zarfam, Mohsen Ghafory-Ashtiany

Inovativna metoda za krivulje inkrementalne dinamičke analize djelomično izoliranih mostova

U radu se predlaže inovativna metoda za određivanje krivulje koja prikazuje približnu inkrementalnu dinamičku analizu djelomično izoliranih mostova uključujući izvod statističkih matematičkih izraza. U konačnici, inovativna je metoda osmišljena na temelju vrijednosti primarne tangencijalne krutosti i granične tangencijalne krutosti djelomično izoliranih mostova. U ovom istraživanju su odabrana dva armiranobetonska mosta autoceste u Sjedinjenim Američkim Državama koji su optimizirani primjenom gumenih ležajeva s olovnom jezgrom. Prikazani postupak može se primijeniti u budućim istraživanjima kako bi se izdvojili probabilistički odzivi djelomično izoliranih mostova uz pomoć jednostavne i učinkovite metode.

Ključne riječi:
djelomično izolirani most, seizmička ocjena, modalna inkrementalna dinamička analiza, inkrementalna dinamička analiza

1. Introduction

Bridges are crucial structures whose uninterrupted operation should be assured, even after catastrophic events such as earthquakes. Currently, bridge design practice widely uses seismic isolation devices for retrofitting existing bridges or for optimised seismic designs of new bridges. The process for isolating the bridges can employ isolators placed under the piers or, alternatively, above the piers. The latter approach has recently received wide attention owing to the relatively lower gravity demands imposed on the isolation devices and resulting optimisation in the design economy. As a result of the shear release in a so-called semi-isolated bridge, an elastic behaviour regime occurs above the isolation interface, whereas the substructure undergoes substantial nonlinearity [1]. One of the most commonly used seismic isolation devices is the lead-rubber bearing (LRB). These devices are highly effective due to the high ductility of the lead core and energy absorption capacity provided by the rubber material. In light of the wide application of semi-isolated bridges, conducting a seismic performance assessment of these bridges has been the subject of numerous recent studies.

One well-known seismic analysis method that accurately accounts for ground motion uncertainties is the incremental dynamic analysis (IDA) (Vamvatsikos and Cornell, 2002). This method derives the relationship between seismic intensity and structural demand and presents it through "IDA curves" [2]. Numerous studies have focused on the IDA curves of bridge structures, seismic zones, and site conditions [3–5]. These studies have used IDA results to identify the ground motion intensities at which the collapses of bridges have occurred [6].

Despite the accuracy and sufficiency of the IDA method, it is associated with a costly numerical process requiring significant time and computing power. To overcome the cost problems of the IDA procedure, researchers have suggested ways to approximate IDA curves through simplification methods proposed for particular classes of structures. Some of these methods rely on analyses performed on equivalent single-degree-of-freedom (SDF) structures. These methods also represent multiple degree-of-freedom (MDF) structures based on the properties of their principal vibration mode [7–9].

One of the earliest examples of such simplification methods is the modal pushover analysis (MPA) proposed by Chopra and Goel (2002) [10], which approximates the intensity-demand relationship by converting structures to equivalent SDF systems based on their modal characteristics. Fragiadakis and Vamvatsikos (2008) fitted a trilinear curve to the pushover curve of an MDF structure in a normalised force-ductility space. They then used numerous IDA results to provide a mapping between the idealised pushover curve and IDA percentiles and implemented the numerical procedure in a computing program called SPO2IDA [11].

Han and Lee (2010) used an MPA to extract the normalised values of yielding and ultimate strengths of an MDF system. They provided formulae for modifying these parameters according to median inelastic and collapse strength ratios obtained through accurate IDA curves of steel moment frame structures [12].

Zarfam and Mofid (2005, 2011) used the concept of the MPA and introduced the modal IDA (MIDA) [13, 14]. The MIDA begins by performing the MPA on an MDF structure and deriving modal force-deformation curves based on which SDF representation of the MDF structure has been defined. The developed equivalent SDF systems are then subjected to separate IDAs. As described in detail below, the application of the MIDA method in evaluating the seismic performance of semi-isolated bridges is also pursued in the current research.

Other researchers have calculated the maximum drift and ductility demands of an MDF building structure by using an equivalent SDF system [15-17].

Chomchuen and Boonyapinyo (2017) represented a single-pier bridge with an equivalent SDF system and obtained its median IDA curve under three artificial earthquakes generated based on Thailand ground motions. They argued that performing an IDA on an equivalent SDF system replaces an IDA on the original structure, reducing computational time and costs [18].

In line with the previous studies and with respect to the importance of semi-isolated highway bridges, the current study aims to provide an innovative methodology for efficient probabilistic seismic assessments of these structures. For this purpose, the MIDA method is adjusted for application on a reinforced concrete highway bridge previously constructed in the United States. This bridge was optimally re-designed using LRB isolators in a previous study by the authors [19]. Performing the MIDA involves constructing an SDF representation of the semi-isolated bridges based on an accurate nonlinear model. An SDF representation of semi-isolated bridges has not been created in previous studies. As such, the provided details and results can help other research studies on this class of structures. Comparing accurate IDA results with approximate MIDAs is regarded as a means for fine-tuning the MIDA procedure and providing a multi-segment process for determining IDA curves. Notably, the MIDA has not yet been used for semi-isolated bridges.

2. Modal incremental dynamic analysis (MIDA) method

In the structural modal analysis process, the effective earthquake force in a mode j is obtained from Rayleigh"s damping, as shown in Eq. (1) [13].

$$P_{j,eff} = -\{\varphi_j\}^T [M][r]\{EQ\ (t)\} \qquad (1)$$

In the above equation, φ_j is the modal shape vector at mode j. To distribute earthquake forces, the vector s is defined as the product of the mass and impact matrices. For mode j, the vector s is called s_j and is calculated using Eq. (2).

$$s_j = \gamma_j [M] \{\varphi_j\} \quad (2)$$

Here, γ_j is the mass contribution coefficient of mode j.
By substituting s_j from Eq. (2) into Eq. (1), the effective force of mode j can be calculated from Eq. (3).

$$P_{j,eff} = -s_j \{EQ (t)\} \quad (3)$$

The MIDA process begins by extracting the mode shapes φ_j and computing $s_j = [M]\varphi_j$ vectors according to Eq. (2). Various s_j vectors are then employed as the modal load patterns under which the structure is subjected to a nonlinear MPA. An appropriate parameter, called the engineering demand parameter (EDP), is selected to represent the response of the system during these analyses. In the case of the bridge structures studied here, the lateral displacement of the deck is considered as the EDP and is plotted against the base shear. Next, the obtained modal pushover curve is idealised using a trilinear curve so that the areas under the actual and idealised curves coincide. The idealised force-displacement curve is then used to represent the structural response at mode j. The SDF system with the derived curve assigned as its hysteretic force-displacement behaviour is called an equivalent modal SDF (EMSDF) system. The mass assigned to the EMSDF is the modal mass at mode j as computed using $\{\varphi_j\}^T[M]\{\varphi_j\}$. The modal damping value is equal to 5 % for each EMSDF system [13].
After establishing all of the EMSDF systems, a set of ground motion records are selected. The IDA is performed on each system by scaling the records to various intensity levels. To scale the records, their intensities are expressed in terms of an appropriately selected intensity measure (IM). The IM-EDP data obtained through the IDA are ultimately plotted against each other and the resulting curve is called the IDA curve. A collapse detection scenario is defined for determining the largest intensity value to which the EMSDF system should be imposed. The EMSDF response is monitored at each intensity level, and the scaling is stopped when a collapse is detected following the current scenario. The median of the IDA curves obtained using different records is extracted and denoted the median IDA curve.
After the derivation of the median IDA (IM-EDP) curves for the various EMSDF systems, these curves are combined using the proposed methods to obtain the maximum proximity between the combined curve and accurate median IDA curve obtained from MDF structure. The combination methods proposed in this study include linear combination using $\gamma_j\varphi_j$ factors and the square root of the sum of the squares (SRSS) method for the results factored with $\gamma_j\varphi_j$. Once the proposed combination method is verified for a structural system, it can be used to simplify the IDA process. Further details regarding the implementation process utilised in this study are presented in the following chapters.

3. Modelling the studied bridges

The bridges studied here are variations of a multi-span highway bridge constructed over the Pilchuck River in Snohomish, Washington, USA. The bridge is supported by abutments at the two ends and by multi-column bents in the middle. This bridge has been previously studied (e.g., [20, 21]) and was optimally designed by the authors using LRB isolators. The LRBs are only placed on top of the middle span piers to isolate the pre-stressed girders of the deck. Neoprene elastomeric plates are used on the abutments (instead of isolators) to support the deck. The geometry of the original variant of the bridge is illustrated in Figure 1 with a pier net height of 4.6 m. To evaluate the effects of the pier height and vibration period on the obtained results, one additional variant with a pier height of 9.6 m is also considered. The preliminary bridge (before optimisation and isolation) investigated in this study is the most common type of bridge constructed throughout the United States according to the National Bridge Inventory, with 30,923 bridges (18.9 % of the total).
The basic material properties used in the bridges are as follows: the shear modulus of the simply-supported bearings (G) is 1 MPa, yield stress of the steel (F_{ys}) is 240 MPa, yield stress of the reinforcement (F_y) is 414 MPa, steel elasticity modulus (E_s) is 2×10^5 MPa, characteristic strength of concrete (f_c) is 28 MPa, and concrete elasticity modulus (E_c) is 25267 MPa. Further details regarding the bridge characteristics can be found elsewhere [20, 21] and are omitted here for the sake of brevity. However, general details are provided below. In the OpenSees model, Concrete01 is used for the unconfined concrete and Concrete02 for the confined concrete. ReinforcingSteel is used to model reinforcements, and Circ. fiber is used for modelling piers. Based on previous studies, quadratic and straight fibres are used for modelling the bents [20, 21]. The deck elements, abutments, and rigid links are modelled with elasticBeamColumn. The translational and rotational stiffness of the pier"s end are modelled with ElasticPP. The soil and piles on the side and under the abutments are modelled with parallel hysteretic materials. A parallel hysteretic material is also used for the elastomeric bearings and dowels. A hysteretic material is used for LRB bearings and shear keys. The impact elements at the deck are modelled with ImpactMaterial.
Owing to the importance of the fibre-based sections of the piers and bents in this research, the details are shown in Figure 2.
Strength degradations are considered in EMSDF models (some elements are mentioned above). Essentially, a three-line model with degradation is used in this research, as shown in Figure 3.
As employed in previous studies [20, 21], the abutment used for this bridge is a pile-bent type. It is assumed that the abutment for this type of bridge uses a 2.4 m back wall height in connection with ten piles. The abutment"s piles are

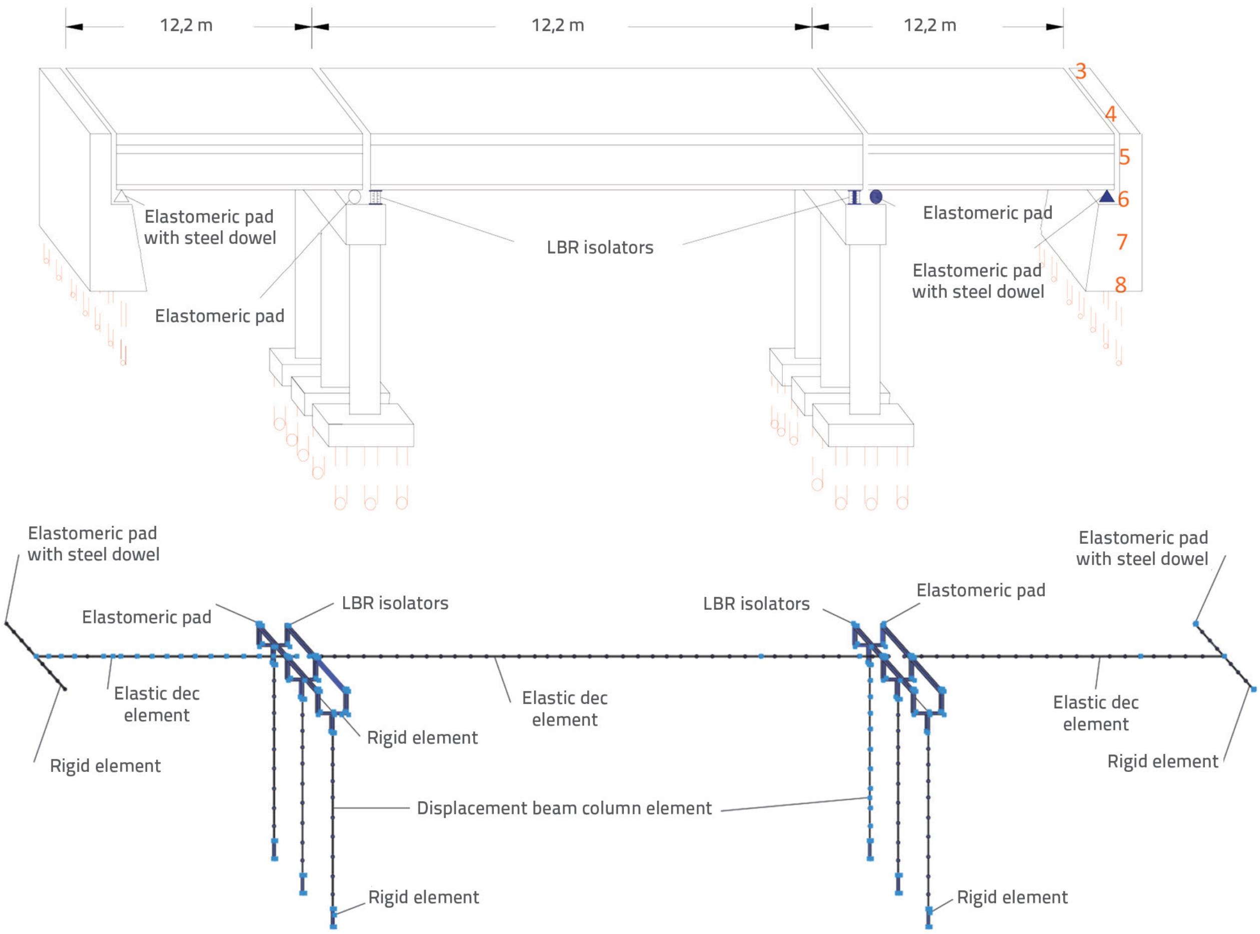

Figure 1. Modelling of the semi-isolated bridge under study

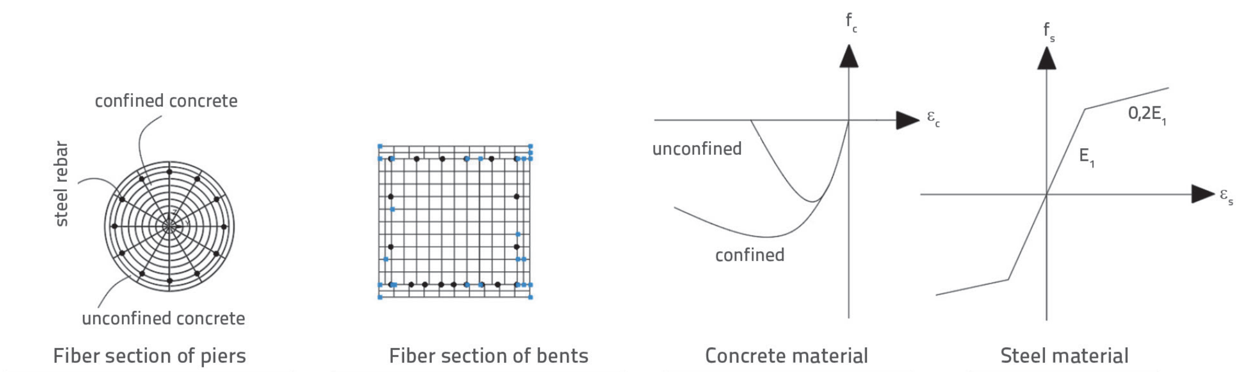

Figure 2. Modelling of the fibre sections for the pier and bent

assumed to operate under both active and passive loading. The Caltrans recommendation of 7 kN per mm per pile is accepted for this study, with an ultimate strength of 119 N per pile (Caltrans, 1990). The behaviour of the piles, however, is not linearly related to the ultimate strength. The initial stiffness decreases with the yield of the soil surface.

The values of the longitudinal, transverse, and torsional modes of the bridge without isolation were validated based on reference model periods [1]. The modal analysis of this model led to first and second vibration periods of 0.62 and 0.42 s, respectively. These values are in agreement with the modal results obtained in previous research [20, 21] and can be regarded as a verification of the model established in this study.

The design of the bridge using LRB isolators was performed in [21] following the limit state specifications of American Association of State Highway and Transportation Officials (AASHTO)-1998 [22] and assuming a soil type D and peak

Table 1. Optimal design dimensions of lead-core rubber bearings (LRBs)

D_c [mm]	**Middle span (bent) LRBs**						**h_c** [m]
	K_{eff} [kN/mm]	**K_u** [kN/mm]	**Q_d** [kN]	**dL** [mm]	**n_r**	**d** [mm]	
900	2.94	20.06	70.1	105	6	350	**4.60**
1000	2.30	17.72	48.68	87.5	7	350	**9.60**

Table 2. Details of hysteresis model of LRBs

h_c [m]	**Force** [N]		**Displacement** [m]		
	F_1	**F_2**	**D_1**	**D_2**	**D_3**
4.60	$7.7931 \cdot 10^3$	22030.5	0.0038841	0.07484	0.15
9.60	$5.4119 \cdot 10^4$	213554	0.00305	0.09304	0.15

ground acceleration, S_S, and S_1 parameters of 0.35 g, 0.7899, and 0.2664, respectively. In addition to the seismic lateral loads, the dead, temperature, vehicle, shrinkage, and brake loads were also considered in the design process and were combined according to AASHTO specifications. The piers were designed based on the American Concrete Institute 318-14 [23] standard. As the design of the gravity load-bearing system (bent girders, pre-stressed deck, and abutments) was unaffected by the isolation system, the related details were taken from designs in previous studies [20]. Compared to the original bridge, the placing of middle-span LRBs leads to increases in the vibration period and structural damping, both resulting in a decrease of the seismic force coefficient. Another important influence of the LRBs is the reduction in the inelasticity level experienced by the isolated bridge.

The optimal design dimensions of the LRBs are shown in Table 1. In this table, d, n_r, Q_d, K_u, and K_{eff} denote the total diameter, number of rubber layers, characteristic strength, elastic stiffness, and effective stiffness of the LRBs, respectively. The D_c parameter is also the diameter of the reinforced concrete piers resulting from design optimisation using genetic algorithms. In addition to the mentioned LRB parameters, the thickness of the upper and lower steel plates is 8 mm, and the thickness of the steel plates between the rubber layers is 3 mm.

The hysteresis model used for the LRBs is presented Figure 3 and the corresponding details are in Table 2.

The methodology used for the nonlinear modelling of the bridge in the OpenSees software is shown in Figure 1. According to Figure 1, the pre-stressed deck is modelled using elastic beam-column elements owing to the effect of the initial compressive force in preventing flexural cracking and nonlinear behaviours of the deck. The three-dimensional behaviours of the supports at the abutment locations tend to impose torsional effects on the deck and out-of-plane bending moments on the piers. To model these effects, the dimension of the deck at its end edge is modelled via the introduction of a rigid beam-column supported on springs reflecting the actions of the neoprene plates and piles. Rigid elements are also used to model the bent dimensions and their effects on reducing the deformable lengths of the deck and piers.

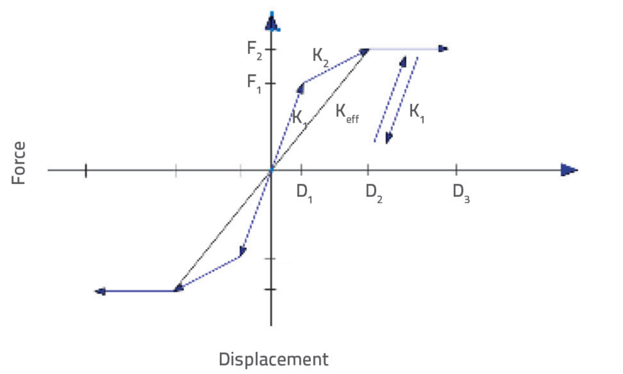

Figure 3. Hysteresis model used for the lead-core rubber bearings (LRBs)

Nelinearni dijelovi modela uključuju stupove i LRB izolatore koji se koriste na ležajnim gredama mosta i ispod ploče. The nonlinear parts of the model include the piers and LRB isolators utilised on the bents and beneath the deck. Fibre displacement-based beam-column elements are used for modelling the nonlinear piers. The displacement formulation used in these elements leads to a loss in accuracy owing to the assumed linear distribution of the curvature along the element length. To overcome this deficiency, the piers are meshed in five segments to achieve an arbitrary distribution of the curvature along with the element. The springs used for modelling the LRBs reflect the LRB behaviours in the horizontal direction and neglect the axial deformations caused by gravity loads.

The pushover analysis results obtained at the longitudinal direction of the bridge are shown in Figure 4 for two pier heights. The control point for the pushover analysis is equal to 15 cm to prevent impacts in the longitudinal direction of the optimised semi-isolated bridges.

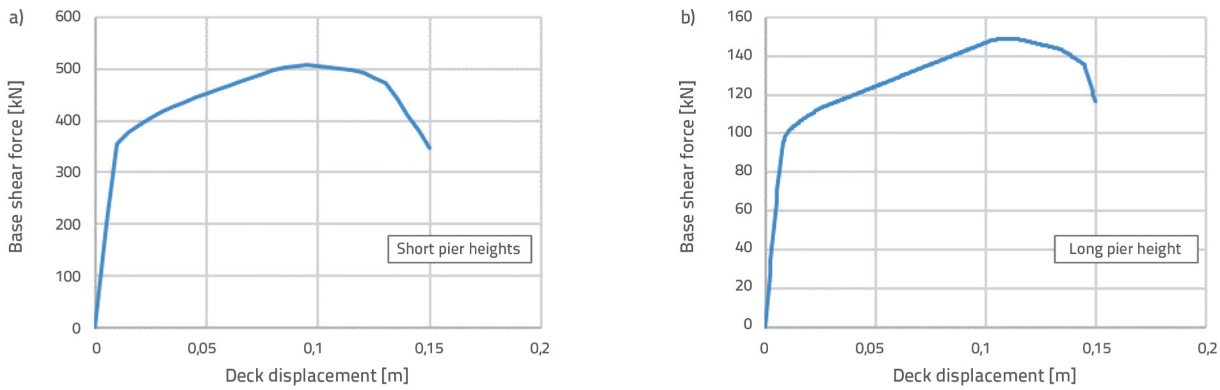

Figure 4. Pushover diagram for semi-isolated bridges with long and short pier heights: a) short pier height; b) long pier height

4. Incremental dynamic analysis (IDA) results

The IDAs are performed by considering the deck displacement and LRB shear deformation as two independent EDPs. The values of these EDPs in two longitudinal and transverse directions are also independently studied to prevent the arguable methods used for identifying the collapse in the case of a three-dimensional response. The 5 %-damped spectral acceleration at the first vibration mode, $S_a(T_1)$, is selected as the IM, and the 44 far-field records [24] recommended by Federal Emergency Management Agency (FEMA) P695 [9] are used to apply the IDAs to the studied bridges. The dynamic analyses are performed unidirectionally in either of the two horizontal directions while neglecting the bridge response in the other direction.

Three criteria are simultaneously considered to capture the occurrence of collapse signalling the stop of the IM scaling procedure. The first criterion accounts for the softening of the IM-EDP curve as a sign of global instability and quantifies it by establishing a limit slope value equal to 20 % of the initial value as recommended by FEMA P695 [24]. The second criterion is based on the displacement limitations dictated by the design standard and construction details. With respect to the construction details, the deck displacement should not surpass a 15-cm distance between the shear key and girder ends to prevent damage to the gravity system and a resulting collapse. Another displacement limit is also posed by the 7.5-cm allowable displacement prescribed for the LRB isolators. The third criterion is the singularity of the stiffness matrix owing to the spread of plasticity throughout the structure and the resulting softening behaviour. Numerically, the identification of this criterion follows the divergence of the analysis after all other causes of non-convergence are thoroughly prevented.

The percentile resulting IDA curves derived using the Hunt-Fill algorithm [2] are illustrated in Figure 5 for the short-pier configurations and by considering various directions and EDPs. For the long-pier bridge, only the percentile IDA curves obtained at the longitudinal direction by considering the deck displacement as the EDP are extracted; the rest of the curves

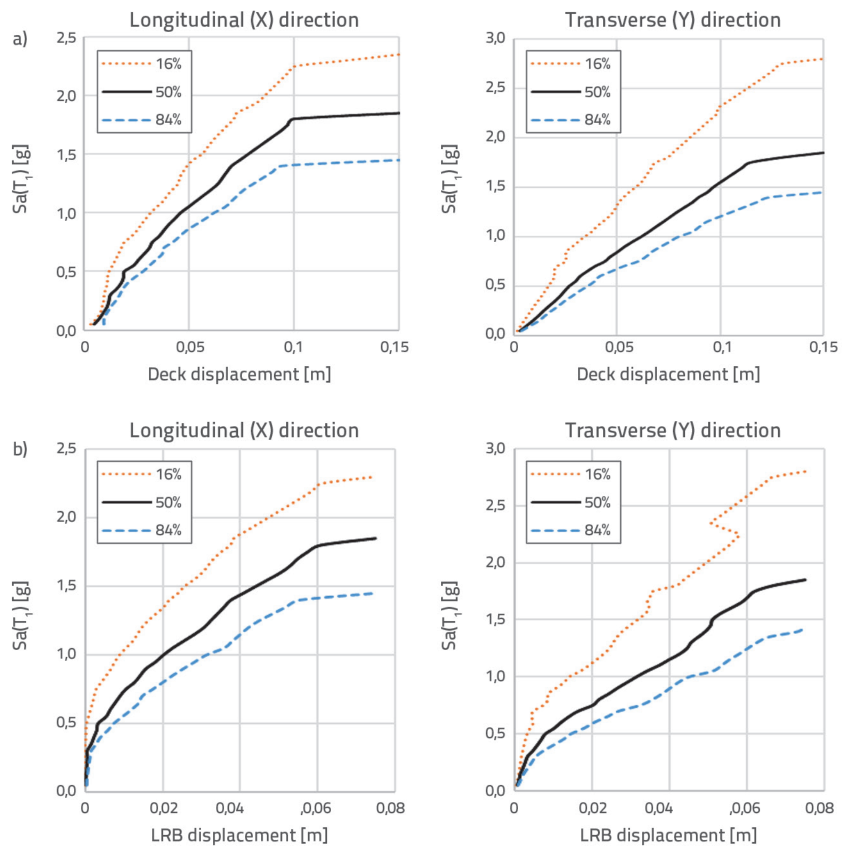

Figure 5. Percentile incremental dynamic analysis (IDA) curves of the short-pier bridge in two horizontal directions considering different engineering demand parameters (EDPs): a) deck displacement; b) LRB displacement

Table 3. Dynamic properties of the considered bridges

Parameters \ The considered bridge	Bridge with short pier			Bridge with long pier		
	Mode 1	Mode 3	Mode 5	Mode 1	Mode 11	Mode 12
Type of mode	Longitudinal	Longitudinal	Longitudinal	Longitudinal	Longitudinal	Longitudinal
Mode period (s)	0,965	0,564	0,513	0,965	0,363	0,275
Modal participation mass ratio	0,733	0,042	0,213	0,648	0,292	0,001
Modal participation factor (tonf.m)	10,96	5,91	1,24	10,8	6,58	1,06
Modal mass (N)	4705964	3492727	4081829	4478078	3463581	3856047

are omitted for brevity"s sake. These curves are illustrated in Figure 6.

Whereas the short-pier configuration collapses mainly owing to the violation of the maximum deck displacement limit, the collapse of the long-pier configuration is occasionally determined by the global instability criterion and corresponding slope limit. Comparing the median results of the two horizontal directions, similar collapse capacities are found. However, the dispersion values indicated by the differences between the percentile curves show a larger value in the transverse direction. This higher scatter of data results from the bridge characteristics in the transverse direction and can negatively affect the reliability of the bridge behaviour in this direction.

As this study aimed to provide a simple method for determining IDA curves for the investigated bridges, the authors tried to be very focused and purposeful in this regard. Therefore, the research was conducted by removing outliers that were not significant to the objective of this study. The bridge selected for this study is a prime bridge that has been widely researched; in this study, we investigated this bridge with isolation. In addition, we utilised the seismic records proposed by FEMA. We attempted to eliminate all sources of uncertainty to focus on a simple method to establish the IDA curves and prevent this article from exceeding its scope. Naturally, however, this approach can be expanded upon in a future work.

Comparing the results related to the various pier heights shows that the median Sa values at which the short-pier and long-pier bridges collapse are 1.9 g and median minus one standard deviation of 1.5 g, respectively. This shows an approximately 20 % reduction in the collapse capacity owing to increased pier height. However, this parameter does not affect the scatter of the observed IDA curves.

As indicated in Figures 5 and 6, the critical direction for determining the IDAs is the longitudinal direction of the semi-isolated bridge, owing to the lower values of the spectral acceleration of the collapse. Therefore, the longitudinal direction of the bridge is used in this study to calculate the MIDA curves.

The dynamic properties of the semi-isolated bridges studied herein are summarised in Table 3. As can be seen in Table 3, over 98 % of the effective modal mass is activated in the short-pier bridge. This number is 94 % for a long-pier bridge.

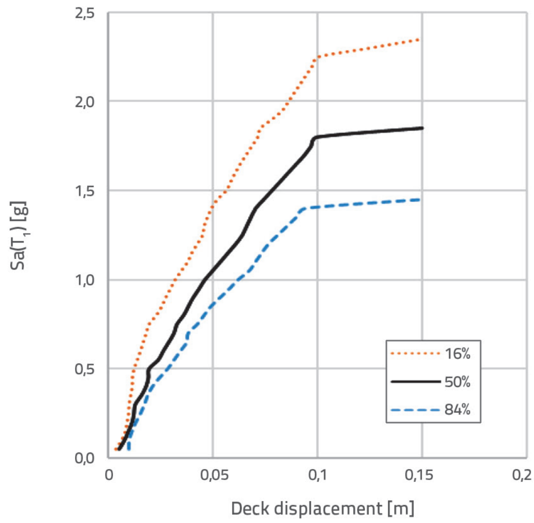

Figure 6. IDA curves obtained for long-pier bridge in longitudinal direction by considering deck displacement as the EDP

5. MIDA results

According to the descriptions presented in Section 2, the MIDA involves the extraction of the modal characteristics of the structure and establishing EMSDF systems, as described in the following section. Upon establishing the EMSDF systems, the IDAs are performed, and the median IDA curves of each EMSDF system are extracted. The median IDAs of various EMSDF systems are combined to obtain the median IDA of the MDF bridge system. The details of this procedure are presented in the following sections.

5.1. Equivalent modal single degree-of-freedom (EMSDF) systems

Three of the major vibration modes are selected for addressing the longitudinal response of the bridges. The neglect of the torsional and transverse modes is because this study focuses on the seismic responses of isolated bridges in their longitudinal direction. This concentration on longitudinal response modes has also been used for building structures by previous researchers such as Chopra and Goel (2002) [10]. The number of selected modes for establishing the EMSDF systems depends on the modal characteristics of the structure being analysed.

Due to the low bridge structure heights and dominance of lower modes, three modes are considered adequate in this study.
After the selection of the mode shapes, they are used to define lateral load patterns under which the static pushover analyses are performed on the bridges.

5.2. EMSDF IDAs

Each EMSDF system is subjected to the IDA procedure using the main components of the ground motion records previously used for performing the bridge IDAs. For conducting the IDAs, the collapse stage is identified using the criteria described in the previous section. Figure 7 presents the median and other percentiles of the IDA curves of the three EMSDF systems established from the short-pier bridge. Figure 8 provides the percentile IDA curves obtained for the EMSDF systems representing the long-pier bridge.
Regarding the Eigen analysis results, Modes 1, 3, and 5 are the first longitudinal modes of the short-pier bridge and are selected for the MIDA process. For the long-pier configuration, the torsional and transverse modes constitute Modes 2–10 of the list, and Modes 1, 11, and 12 are selected for representing the longitudinal behaviour.

5.3. Combining the EMSDF IDAs

To generate the MIDA curves, the median IDA curves obtained for the various modes are combined. Two combination methods are utilised for this purpose. The first approach follows the method employed by the MPA [18] and combines the modal results using the SRSS method.
The second approach uses an algebraic summation based on the characteristics of the modal responses, as presented in Section 3. An EDP-based approach is utilised to numerically combine the median IDA curves obtained from the EMSDF systems. In this approach, constant deck displacement values ranging from zero to the maximum observed displacement are considered in 0.01-m intervals (shown with dots for a better display). The IM values corresponding to the generated EDP values are then extracted by interpolating the values on the various MIDA curves. The extracted IM values are then combined using either of the described combination methods. Each combined IM value is

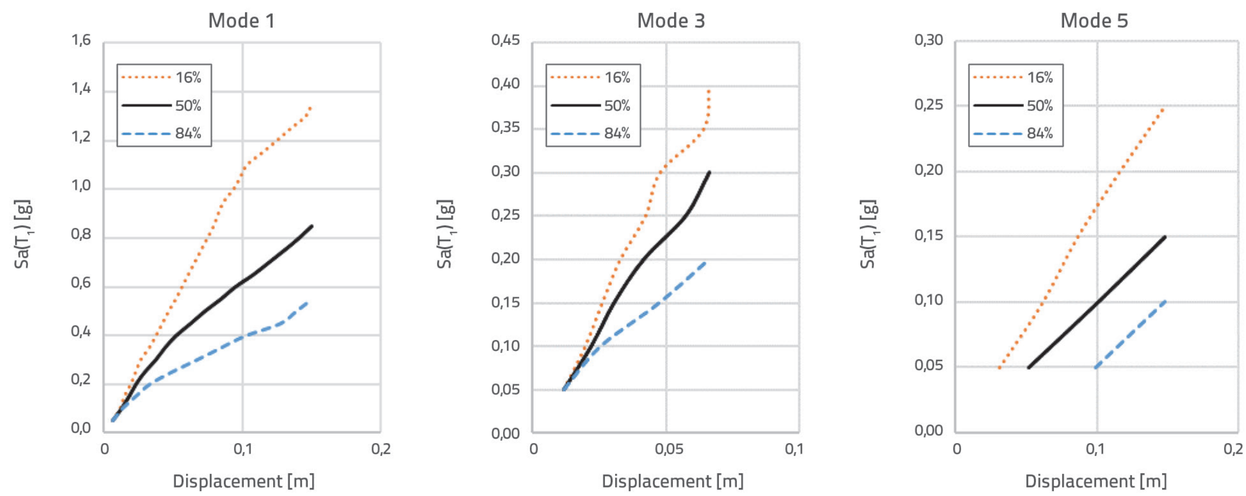

Figure 7. Percentile IDA curves of equivalent modal single degree-of-freedom (EMSDF) systems representing the short-pier bridge

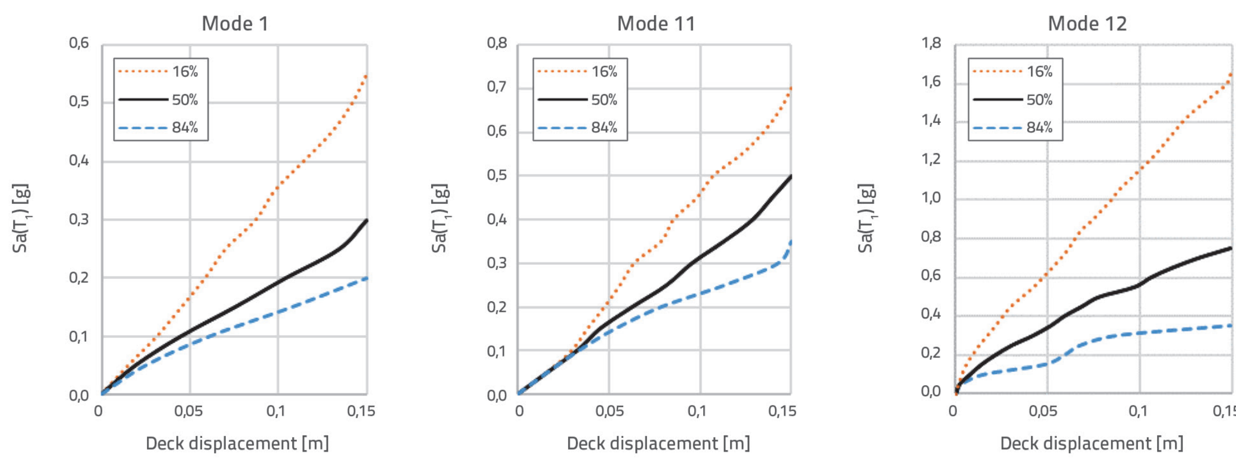

Figure 8. Percentile IDA curves of EMSDF systems representing the long-pier bridge

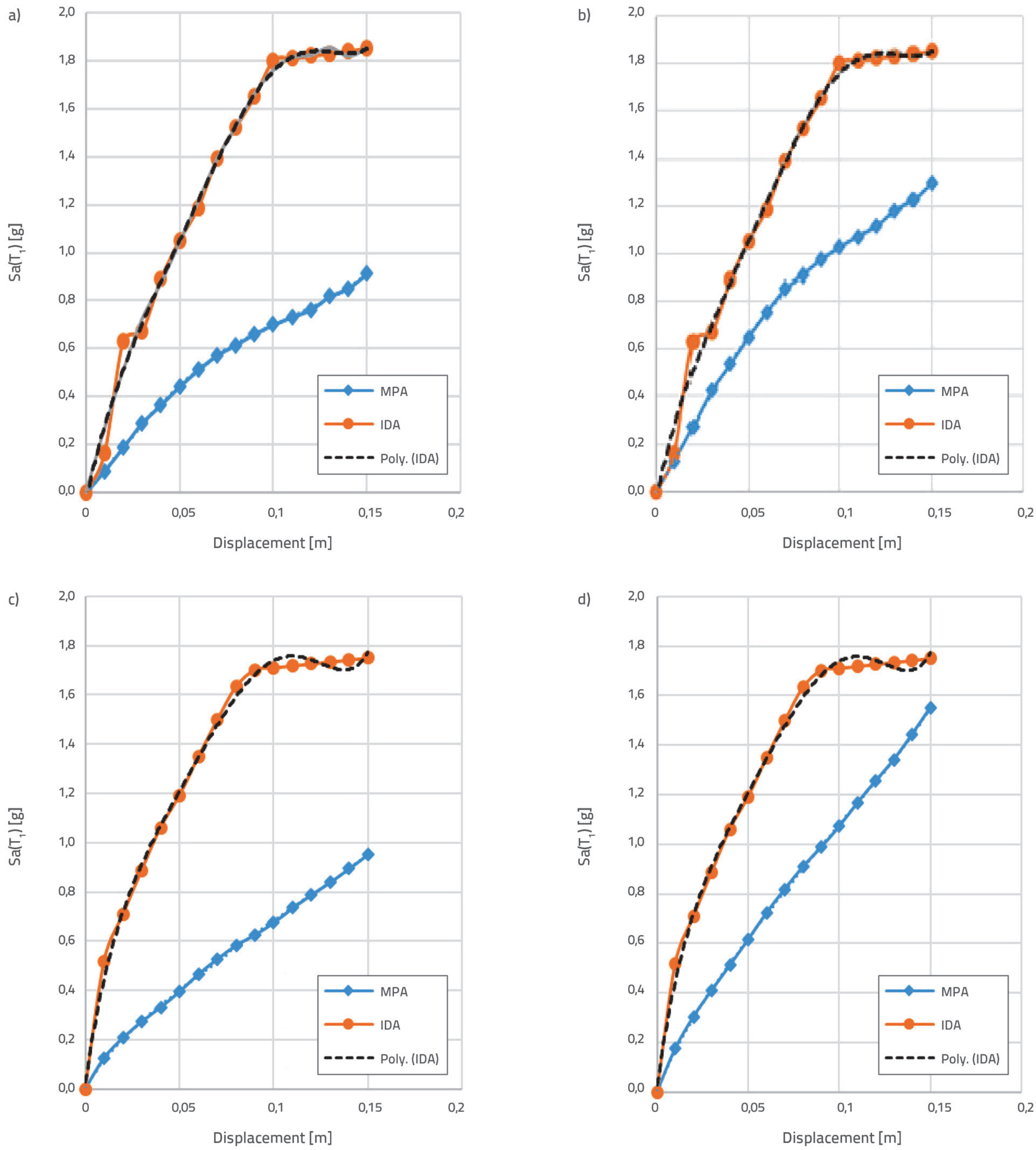

Figure 9. Comparison between original IDA, interpolated IDA, and modified IDA (MIDA) curves for a) short-pier bridge, square root of the sum of the squares (SRSS) combination; b) short-pier bridge, algebraic summation; c) long-pier bridge, SRSS combination; d) long-pier bridge, algebraic summation

plotted against the corresponding EDP value to form a point on the combined IDA curve. The IM values, as interpolated using the accurate IDA curve of the MDF model (called the segmented IDA curve), are shown in Figure 9. The combined MIDA curves obtained using the various combination methods are also shown in this figure for either of the two bridges. In Figure 9, the blue lines are the curves determined in the MIDA by the two procedures (algebraic summation and SRSS combination). The orange lines are the median exact IDA curves determined by the analysis. The dashed black lines (referred to as "Poly.(IDA)") are also related to the regressions given in Equations 4 and 5 and Tables 4 and 5.

A regression analysis is performed to formulate the correlation between the combined MIDA curves and the accurate IDA curves generated in the previous section. For this purpose, a scale

Table 4. Regression coefficients obtained for computing scale factor at various engineering demand parameter (EDP) values of the incremental dynamic analysis (IDA) curves combined using square root of the sum of the squares (SRSS) method

c_{16}	c_{15}	c_{14}	c_{13}	c_{12}	c_{11}	c_6	c_5	c_4	c_3	c_2	c_1	The considered bridge
0.0014	9.273	35.581	1170.5	7060	11863	0.0349	37.302	680.98	10973	82654	216256	Short- pier bridge
-0.0051	12.757	-181.96	-2376.2	-15254	-37302	-0.0314	51.786	1163.9	17495	126167	329084	Long-pier bridge

Table 5. Regression coefficients obtained for computing scale factors at various EDP values of the IDA curves combined using algebraic summation

c_{16}	c_{15}	c_{14}	c_{13}	c_{12}	c_{11}	c_6	c_5	c_4	c_3	c_2	c_1	The considered bridge
0.0008	12.993	80.732	2127.8	12777	23066	0.0349	37.302	680.98	10973	82654	216256	Short- pier bridge
-0.0044	18.062	-212.73	-2723.9	-17801	-45381	-0.0314	51.786	1163.9	17495	126167	329084	Long-pier bridge

factor (SF) is defined at a given EDP by dividing the accurate IM value over the modal value (Eq. (4)).

$$S_{a\text{-MDF}} = SF \cdot S_{a\text{-EMSDF}} \tag{4}$$

The relationship between the computed SF and EDP values is then expressed using a regression equation in the form of Eq. (5). In this equation, x is the EDP value, c1 to c6 are the regression coefficients at the numerator, and c11 to c16 are the coefficients at the denominator.

$$SF = (c_1x^5-c_2x^4+c_3x^3-c_4x^2+c_5x-c_6)/(-c_{11}x^5+c_{12}x^4- -c_{13}x^3+c_{14}x^2+c_{15}x-c_{16}) \tag{5}$$

The values of the regression coefficients obtained for the two short-pier and long-pier bridges are presented in Table 4 for the MIDAs combined using the SRSS method. The regression coefficients obtained using the IDAs combined by algebraic summation are presented in Table 5.

5.4. Innovative multi-segment method for combining the EMSDF IDAs

Owing to the behavioural modes not reflected by the EMSDF systems, the IDA curves obtained using these systems do not accurately represent certain characteristics of the accurate IDA curves obtained using the MDF model. The behavioural aspects lacking in the EMSDF systems include the second-order p-delta forces (not included owing to the zero dimensions of these systems) and ignorance of the rotational degrees of freedom. Furthermore, the selected EMSDF systems do not include all of the vibration modes of the complete MDF system. The neglect of the EMSDF systems corresponding to the higher modes is, therefore, another cause of the differences between the accurate and MIDA curves. Nevertheless, it should be emphasised that only the first three structural vibration modes are being considered. Over 20 structural vibration modes are usually considered in the longitudinal and transverse directions in bridge design.

Based on Eq. (3), the earthquake force can be considered as a combination of modal forces $p_{j,eff}$ at any instance of time. To obtain the response of an MDF structure under an earthquake, its response under the various modal forces can be computed and linearly combined, provided that the system behaves in the linear range. The modal responses cannot be linearly combined for nonlinear systems, and appropriate nonlinear equations are required to obtain the complete system response. The key is deriving these equations so that the limit state capacity of the system can be accurately predicted via a combination of modal responses. According to Eq. (3), the effective modal force is a time-varying scale of the modal vector s_j. Thus, analysing the structure under the full range of SFs, starting from a linear response and ending in total collapse, can help in predicting the nonlinear dynamic modal response.

To address these deficiencies through an empirical method, an alternative method is proposed for estimating the accurate IDA curve using the modal curves. This innovative approach presents a simple and efficient method for obtaining an accurate IDA curve from the results as calculated by the MIDA method in this study. By numerically reviewing the research results, the values listed in Table 6 are determined and proposed for the bridges considered in this study. In addition, the previous point-to-point mapping between the modal and accurate IDA curves is modified according to two regions, as discussed below:

1. An initial region starting from δ = 0, in which the spectral values are amplified by the values listed in Table 6 and ending with the point with the slope listed in Table 6
2. A collapse plateau starting from the point with the slopes mentioned in Table 5 and continuing towards infinity with a zero slope.

In the initial region, the coefficient values for the SRSS and algebraic summation methods are presented in Table 6 and Figure 10, respectively. The end of this region is denoted by the point $\delta = \delta_u$; this can be identified as the point at which the IDA curve deviates from the initial curve.

Table 6. Values of the scale factor at the first region (SF_h) and slope

Pier height	SF_h		Slope
	SRSS combination	Algebraic summation	
Short-pier	2,50	1,60	0,35
Long-pier	2,85	2,00	0,45

In the initial region, a constant SF SF_h is used for estimating the accurate IDA curve by scaling the IM values of the combined modal curves. The value of SF_h depends on the pier heights and response combination method utilised according to Table 6. For the determination of δ_u value at which the collapse plateau starts, the softening of the modal IM-EDP curve is considered by establishing a slope value. The slope value can be obtained by a comparison between combined modal IM-EDP curves and collapse plateau of the accurate IDA curves. As a result, slope values equal to 0.35 and 0.45 of the initial slope are recommended for bridges with short and long piers, respectively.

$$S_{a\text{-}MDF} = SF_h \cdot S_{a\text{-}EMSDF} \quad (6)$$

Notably, when using the methods in Sections 5.3 and 5.4 of this paper, the approximate MIDA curves are placed on the exact IDA curves.

To conduct this research, it was necessary to perform an accurate IDA. However, based on the suggestions from the numbers shown in Table 6, for bridges similar to the important semi-isolated optimised bridges considered in this study, there is no need to perform the accurate IDA, as the results can be determined from the values listed in Table 6.

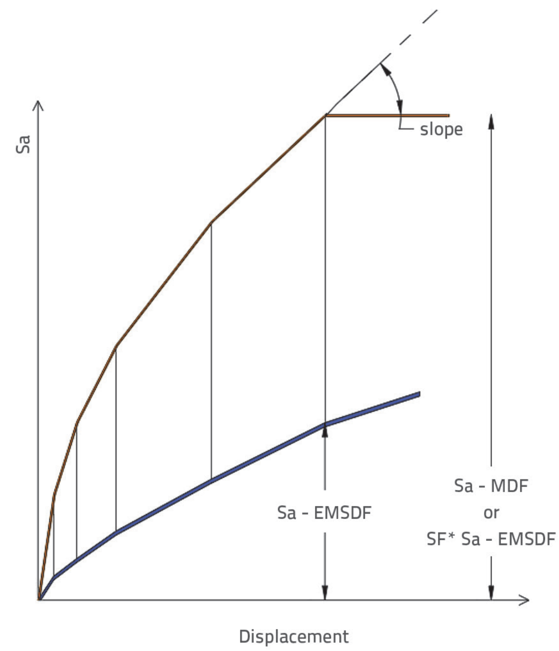

Figure 10. Innovative multi-segment method for combining the IDAs

6. Conclusions

In this study, a seismic performance assessment of semi-isolated RC bridge structures was initially conducted by incorporating an accurate IDA procedure. A MIDA was performed to establish an efficient simplified method to account for ground motion uncertainties with lower analysis costs and to approximate the median IDA curves of MDF structures.

The two combination methods (SRSS and algebraic summation) could only approximate the MDF IDA curve before the collapse plateau. To predict the collapse plateau, an innovative multi-segment combination method was proposed for precisely approximating the IDA of the semi-isolated bridge according to its full range of responses.

REFERENCES

[1] LRFD Seismic Analysis and Design of Bridges (Reference Manual), Publication No. FHWA-NHI-15-004, U.S. Department of Transportation, (2014)

[2] Vamvatsikos, D., Cornell, C.A.: Incremental dynamic analysis." Earthquake Engineering and Structural Dynamics, 31 (2002) 3, pp. 491-514.

[3] Zhang, J., Huo, Y.: Optimum isolation for highway bridges using fragility function method, The 14th world Conference on Earthquake Engineering (14WCEE), October 12-17, 2008, Beijing, China.

[4] Rahman Bhuiyan, A., Shahria Alam, M.: Seismic Fragility Assessment of a Multi-Span Continuous Highway Bridge Isolated by Shape Memory Alloy Restrainer and Lead Rubber Bearing, The 15th world Conference on Earthquake Engineering (15WCEE), (2012), Lisboa, Portugal.

[5] Yön, B., Öncü, M.E., Calayır, Y.: Effects of seismic zones and site conditions on response of RC buildings. Gradevinar, 67 (2015) 6

[6] Jamie, E., Padgett, J.E., DesRoches, R.: Methodology for the development of analytical fragility curves for retrofitted bridges, Earthquake Engineering and Structural Dynamics, 37 (2008) 8, pp. 1157-1184.

[7] Han, S., Chopra, A.K.: Approximate incremental dynamic analysis using the modal pushover analysis procedure." Earthquake Engineering and Structural Dynamics, 35 (2006), pp. 1853-1873.

[8] Dolšek, M., Fajfar, P.: Simplified nonlinear seismic analysis of infilled reinforced concrete frames, Earthquake Engineering and Structural Dynamics., 34 (2005) 1, pp. 49-66.

[9] Vamvatsikos, D., Cornell, C.A.: Direct estimation of the seismic demand and capacity of multi-degree-of-freedom systems through incremental dynamic analysis of single degree of freedom approximation, Journal of Structural Engineering, 131 (2005) 4, pp. 589-599.

[10] Chopra, A.K., Goel, R.K.: A modal pushover analysis procedure for estimating seismic demands for buildings, Earthquake Engineering and Structural Dynamics, 31 (2002), pp. 561-582.

[11] Fragiadakis, M., Vamvatsikos, D.: Approximate seismic performance uncertainty estimation using static pushover methods, The 14th World Conference on Earthquake Engineering October 12-17, 2008, Beijing, China.

[12] Han, S. W., Lee, T. S.: Approximate incremental dynamic analysis using modal pushover, 7th International Conference on Urban Earthquake Engineering (7CUEE) & 5th International Conference on Earthquake Engineering (5ICEE) March 3-5, 2010, Tokyo Institute of Technology, Tokyo, Japan.

[13] Zarfam, P., Mofid, M.: On the modal incremental dynamic analysis of reinforced concrete structures, using a trilinear idealization model, Journal of Engineering Structures, 33 (2011) 4, pp. 1117-1122.

[14] Mofid, M., Zarfam, P., Raiesi Fard, B.: On the modal incremental dynamic analysis, The Structural Design of Tall and Special Buildings, 14 (2005) 4, pp. 315-329

[15] Li, H.N., Qu, C., Huo, L.S., Nagarajaiah, S.: Equivalent bilinear elastic single degree of freedom system of multi-degree of freedom structure with negative stiffness, Journal of Sound and Vibration, 365 (2016), pp. 1-14.

[16] Jalilkhani, M., Manafpour, A.R.: A Simplified Modal Pushover Analysis-based Method for Incremental Dynamic Analysis of Regular RC Moment-resisting Frames . International Journal of Engineering, TRANSACTIONS B: Applications, 31 (2018) 2, pp. 196-203.

[17] Bojórquez, E., Bojórquez, J., Ruiz, S.E., Reyes-Salazar, A., Velázquez-Dimas, J.: Response transformation factors for deterministic-based and reliability-based seismic design, Structural Engineering and Mechanics, 46 (2013) 6.

[18] Chomchuen, P., Boonyapinyo, V.: Incremental dynamic analysis with multi-modes for seismic performance evaluation of RC bridges, Engineering Structures,132 (2017), pp. 29-43

[19] Ganjehei, H.: Seismic design optimization of Isolated RC deck road bridges based on Genetic Algorithm using Monte Carlo Simulation and MIDA, Ph.D. Thesis, Department of civil engineering, Science and Research Branch, Islamic Azad University, Tehran, Iran, 2021.

[20] Hwang, H., Jernigan, J.B., Lin, Y.W.: Evaluation of seismic damage to Memphis bridges and highway systems, Journal of Bridge Engineering, 5 (2000) 4, pp. 322-330.

[21] Bryant, G.N.: Analytical Fragility Curves for Highway Bridges in Moderate Seismic Zones, Georgia Institute of Technology, 2005.

[22] AASHTO, LRFD Bridge design specifications: American Association of State Highway and Transportation Officials: Washington, D.C., 1998

[23] ACI, Building code requirements for structural concrete, in ACI 318-14, 2014, American Concrete Institute.

[24] FEMA P695: Quantification of Building Seismic Performance Factors, Federal Emergency Management Agency, June 2009.